EMITTER International Journal of Engineering Technology
Vol. 11, No. 1, June 2023, pp. 60~75
DOI : 10.24003/emitter.v11i1.758

Planar Microwave Sensor with High Sensitivity for Material Characterization Based on Square Split Ring Resonator (SSRR) for Solid and Liquid

Maizatul Alice Meor Said[1], Zahriladha Zakaria[1], Mohamad Harris Misran[1], Mohd Azlishah bin Othman[1], Redzuan Abdul Manap[1], Abd Shukur bin Jaafar[1], Shadia Suhaimi[2], Nurmala Irdawaty Hassan[3]

[1]Centre for Telecommunication Research & Innovation (CeTRI),
Fakulti Kejuruteraan Elektronik dan Kejuruteraan Komputer (FKEKK),
Universiti Teknikal Malaysia Melaka (UTeM), Melaka, Malaysia.
[2]Faculty of Business, Multimedia University, Melaka, Malaysia.
[3]Electrical & Electronic Engineering Programme School of Engineering and Physical Sciences, Heriot-Watt University Malaysia, Putrajaya, Malaysia
Corresponding Author: maizatul@utem.edu.my

Received January 5, 2023; Revised March 11, 2023; Accepted May 13, 2023

Abstract

Microwave resonator sensors are the most extensively used sensors in the food industries, quality assurance, medical, and manufacturing. Planar resonant technique is chosen as the medium for characterizing dielectric properties of material due to its compact in size, low cost and easy to fabricate. But these techniques have a low Q-factor and little sensitivity. This work uses the perturbation approach to overcome this technique's flaw, which is that Q-factor and resonant frequency are affected by the resonator's dielectric properties. This suggested sensor operated at 2.5GHz between 1GHz and 4GHz for material characterisation of solid and liquid samples. These sensors were constructed on a substrate made of RT/Duroid Roger 5880, which has a copper layer that is 0.0175 mm thick and has a dielectric constant of 2.2. This square split ring resonator (SSRR) sensor thus generates narrower resonant, low insertion loss, and a high Q-factor value of 430 at 2.5GHz. The SSRR sensor's sensitivity is 98.59%, which is higher than that of past studies. The application of the suggested sensor as a tool for material characterisation, particularly for identifying material attributes, is supported by this findings.

Keywords: Material Characterization, High Q-Factor, Microwave Resonator Sensor, Solid and Liquid Sample.

1. INTRODUCTION

The microwave sensor has become the most prominent sensor for material characterization in the food manufacturing, quality assurance, medical applications, and industrial settings [1–3]. The presence of specific components in food items can influence consumers and cause diseases like allergies, poisoning, and cancer, thus it is crucial that food products take health and safety precautions to protect the health and wellness of consumers [3]. Therefore, it's crucial to verify both safety and quality of goods before selling them to customers, especially for things like beverages and cooking oils [3]. The two types of methodologies for material characterization are resonant methods and non-resonant methods. Broadband methods are another name for non-resonant techniques. Non-resonant methods are typically utilised for electromagnetic properties across a frequency range, while resonant techniques are frequently used to precisely comprehend a single frequency or a small number of frequencies of dielectric qualities [4].

One of the prospective methods for a very accurate examination of the characteristics of dielectric materials at a specific or few frequencies is the microwave resonant approach. Coaxial, waveguide, and dielectric resonators have all been employed in the past to reliably and precisely characterise materials [5]. However, the conventional resonator sensor is typically large, costly to construct, and needs a lot to detect the sample of the object being examined [5–8]. Planar resonant techniques have increased in popularity recently due to their benefits of being portable, inexpensive, and easy to build [9–12]. However, the breadth of material characterization is limited by this method's weak sensitivity and Q-factor values.

The purpose of the current research was to create an improve microwave sensor with compatibility, low cost, a straightforward design, simple handling, a higher Q-factor, improved accuracy, and sensitivity in order to address these problems. The attributes that govern a material's electrical nature are thus determined by permittivity, which is extremely important. As permittivity increases from low to high, the resonance frequency swings to the left [13,14].

2. RELATED WORKS

Early in the 1950s, the domain of characterisation of microwave frequency material properties was formed. A remarkable idea for novel measurement techniques has been devised. Numerous approaches have been devised to describe the dielectric properties of materials [15–18]. Rapid industrial development currently calls for a precise material characterization measurement that satisfies the requirements of being highly accurate and economical, serves as a sensitivity device, and is small enough to fit in many different important applications, including the food and beverage industry and bio sensing [3,19,20].

Despite the numerous applications, science works to understand why some materials act the way they do. A material's response to electromagnetic (EM) fields is significantly influenced by the polarity of its constrained electrons. Correlations between material properties and EM fields have resulted in a full understanding of EM materials and their usage in science by applying both theoretical and scientific methodologies. Applications involving material characterization play a big part in the requirements of the device that may supply such essential information. This part comprises the philosophy that underpins a key design feature of the proposed sensor and explains the concept that supports it. It will evaluate the elements that must be considered in order to design a method that would lead to a high accuracy and reasonably priced microwave sensor for material characterization based on previous development projects and breakthroughs.

The non-resonant and resonant forms of microwave measurements for materials characterization are depicted in Figure 1. Non-resonant approaches can be used to evaluate the dielectric properties over a broad frequency range, but resonant techniques offer more exact knowledge of the dielectric characteristics over a particular range of frequencies or a specific frequency [4]. The resonant approaches, such as the resonator method and the resonator perturbation method, are contrary to the non-resonant techniques, which include reflection methods and transmission/reflection methods [21].

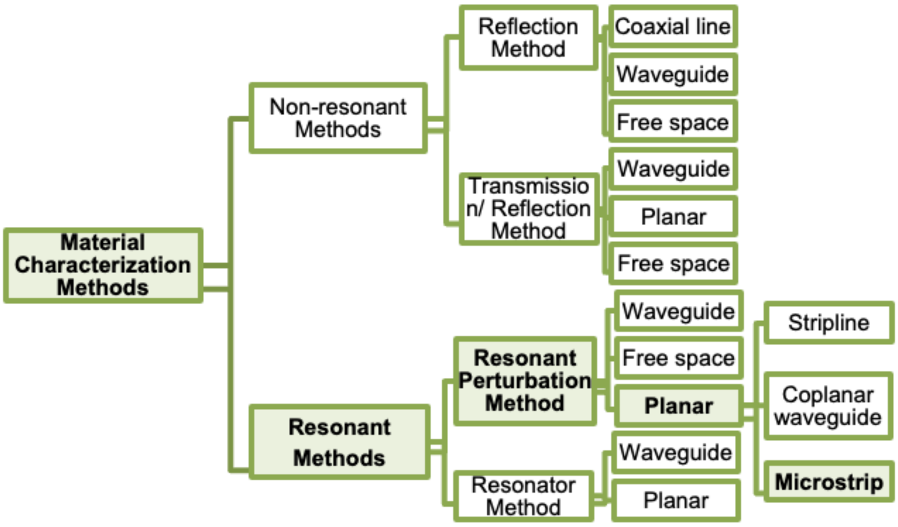

Figure 1. Classification of the material characterization method

3. ORIGINALITY

In this study, we suggest designing a microstrip planar resonator sensor that use the SRR method because it can provide more unique designs with good measurement sensitivity and show great potential as a high-frequency integrated circuit option. In addition, the SRR structure has a straightforward design that is simple to implement and visibly economical. The physical characteristics of the sample have a significant impact on the procedures used to maximise the overall effectiveness of the proposed sensor. Most sensors are primarily interested in determining the dielectric characteristics of one particular type of material, such as solid, liquid, semi-solid, or gas materials. But this study offered a sensor capacity that can assess the dielectric characteristics of two different sample types solid and liquid using a single resonator sensor.

The perturbation method (PM) appears to be the best resonant cavity approach [22,23]. The resonance frequency of a cavity is frequently altered by changing the form of the cavity. The procedure of material perturbation, often referred to as the method of cavity disruption, involves placing the sample within the cavity, which modifies the cavity's resonance frequency and quality factor. Wall-loss perturbation was then used to identify the surface resistance of conductors by replacing a section of the empty wall with the tested material. This method is typically applied to small samples. The samples interferes with the area's propagation, causing the reliability parameter of the resonator to shift to lower Q-values and lower frequencies in the resonant frequency range. The frequency resonance used to measure the characteristics of materials is impacted by the interference between the sample and electrical field energy deposited [24].

4. SYSTEM DESIGN

For the development of sub-wavelength magnetic metamaterials resonators, the split ring structure is a basic geometry. The design strategy has become so alluring in the growth of microwave frequencies. The resonant frequencies of the ring structure will be determined analytically, and any modifications to this constitution will be verified experimentally. In order to determine the best architectural design for the single split ring resonator, the mathematical formula will be driven by the resonant frequency. Figure 2 illustrates the fundamental geometry idea that was employed for this investigation which the parameters consists the width, w, the length, l, the height (thickness), h, and the gap width, g. The inductor, (L) and capacitor, (C) can be used to describe the capacitance and inductance values of the split ring resonator.

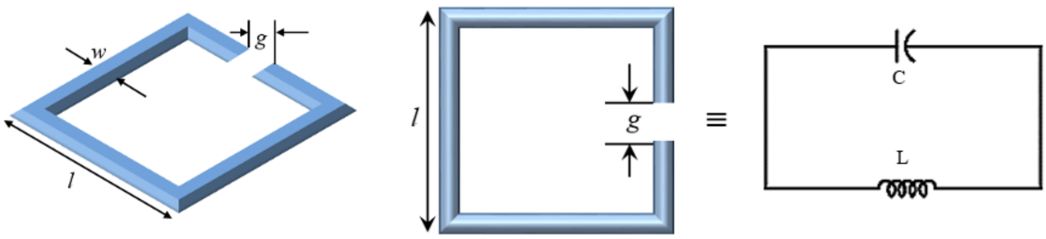

Figure 2. The basic concept of geometry

The split-ring resonator calculation is used to predict the geometric structure in the beginning stages of the sensor design by using equations (1)-(3) [25,26]. A microwave microstrip resonator and a planar ring resonator make up the sensor architecture. The proposed resonator's resonance frequency is dependent on the length of the microstrip line. This resonator is a half-wavelength resonator, and the following formula equations can be used to compute the length of the microstrip line connected to the resonance frequency:

$$l = \frac{c}{2\pi\sqrt{\varepsilon_{eff}}} \times \frac{1}{f_o} \quad (1)$$

$$\frac{w}{d} = \frac{8e^A}{e^{2A}-2} \quad (2)$$

A for area

$$\varepsilon_{eff} = \frac{\varepsilon_r+1}{2} + \frac{\varepsilon_r-1}{2}\left[\frac{1}{1+12\frac{h}{w}}\right] \quad (3)$$

A parallel RLC resonant circuit can adequately characterise the SRR architecture as we go toward design development. The gap capacitance corresponds to C, while the value of L relies on the ring's transmission line. Equation (4) can be used to obtain the resonance frequency.

$$f_r = \frac{1}{2\pi\sqrt{LC}} \quad (4)$$

When compared to other available structures, it is anticipated that the folded arm construction will create a narrower band and a sharper slope, exposing its high Q nature. The Q-factor, also known as a resonant circuit's quality factor, is a dimensionless quantity that represents the energy losses within the resonance element. It reveals the relationship between the resonator's bandwidth and its fundamental frequency. Equation (5) can be used to represent the Q-factor, where f_o is the central resonance frequency and BW is the bandwidth at 3 dB with respect to the smallest transitions [27–29].

$$Q = \frac{2f_o}{BW} \quad (5)$$

4.1 Design using Computer Simulation Technology (CST)

In this research study, the proposed sensor is constructed with a 2.5GHz working frequency. Figure 3 illustrates the construction of a square SRR at a single port system with a single patch structure.

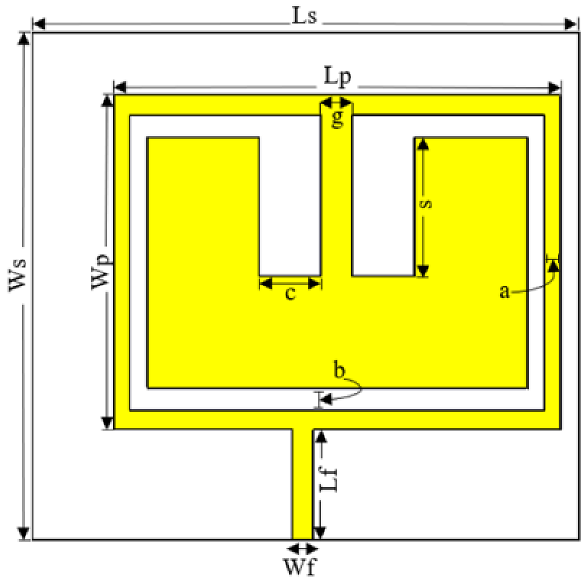

Figure 3. Proposed SSRR architecture

The ground plane and patch are made of annealed copper, and the substrate for the microwave resonator sensor is made of Roger 5880. Table 1 displays the parameter's value after optimization based on a common equation of designation for a microwave resonator sensor.

Table 1. Parameter Specifications

Parameter	Design Value
Substrate	Roger 5880
Operating Frequency	2.5 GHz
Substrate height (hs)	0.787 mm
Substrate permittivity	2.2
The thickness of copper (t)	0.0175 mm
Substrate Length (Ls)	65 mm
Substrate Width (Ws)	60 mm
Length of feedline (Lf)	13 mm
Width of feedline (Wf)	2.45 mm
Width patch (Wp)	39.23 mm
Length patch (Lp)	52.31 mm
Gap patch (g)	3.71 mm
Slot length (s)	18.96 mm
Slot width (c)	7.32 mm
Width 1 (a) and Width 2 (b)	1 mm

Figure 4 showed that during the simulation using computer simulation technology (CST), the material under test (MUT) was positioned on top of the copper patch. As shown in Figure 5, the sample is put on an electric field with the highest intensity. The material under test (MUT) is put at the high of the electric field at the top of copper tracks, in the middle between patch and feedline, as illustrated in Figure 5, and this area has a high concentration of electric fields. The identical steps will be followed in the exact same spot while setting up microfluidic case for liquid samples. These studies will examine two types of materials: solid samples and liquid samples with uniform relative permittivity values. The outcomes of the simulation are compared to a theoretical model of dielectric characteristics at microwave frequencies.

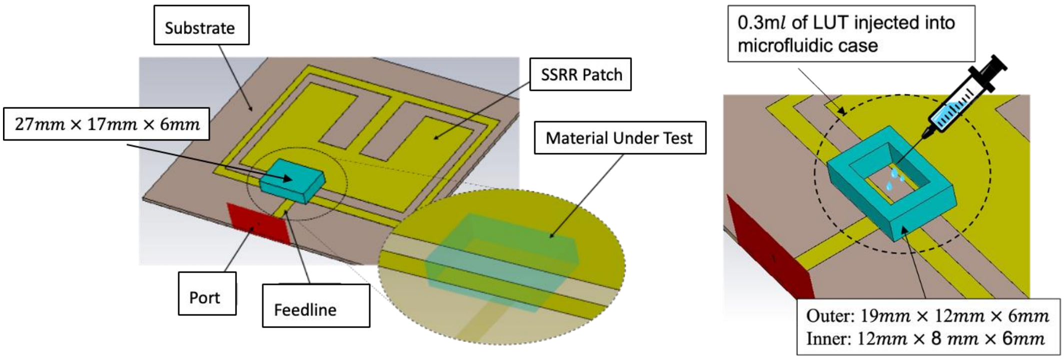

Figure 4. Location of MUT on CST

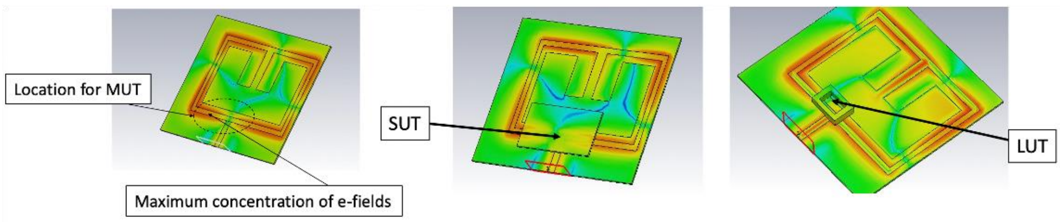

Figure 5. Location of MUT on high concentration region

4.2 Calibration using Vector Network Analyzer (VNA)

A vector network analyzer (VNA) was used to evaluate the microwave resonator sensor and determine its S_{11} return loss between 1 GHz and 4 GHz. The 50Ω SMA-Connector connector on the sensor connects the VNA to the sensor through the two probe stations. This research employed Roger 5880, that has a thickness of 0.787mm, a dielectric constant of 2.2, and a tangent loss of 0.0009, as the substrate for this microwave resonator sensor. A liquid sample of a 100% pure solution with a volume of 0.3ml is been injected into the microfluidic box, while each solid sample with a size of 27mm x 17mm is been placed over of the copper patch. The test for both the solid under test (SUT) and liquid under test (LUT) was performed at the same ambient temperature of 25 °C. The same testing approach is used for materials that are evaluated at an operating frequency of 2.5 GHz in the frequency range of 1GHz to 4GHz for both solid and liquid forms of the material. Figure 6 displays the measurement set-up using the Vector Network Analyzer (VNA).

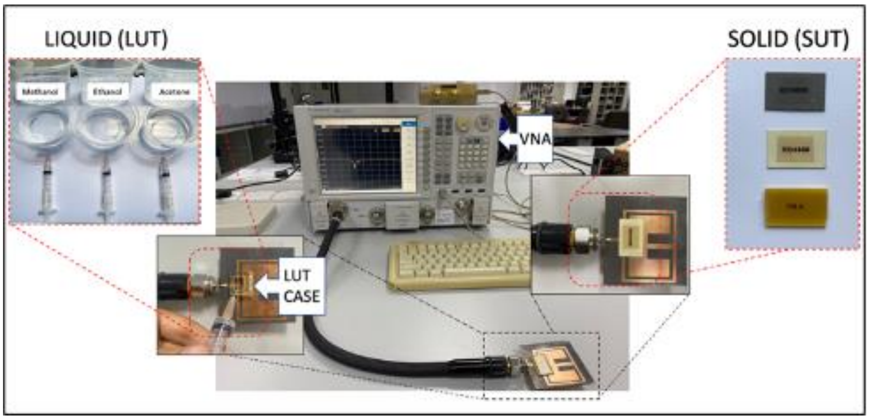

Figure 6. Measurement setup using VNA

5. EXPERIMENT AND ANALYSIS

5.1 Q-Factor Analysis

The microwave resonator sensor's accuracy was evaluated using resonant frequency shifting. A graph comparison of experimental and predicted outcomes without a sample is displayed in Figure 7. As illustrated in Figures 8 for simulated results and Figure 9 for real outcomes, the resonance frequency is moved to a lower frequency by increasing the sample's permittivity value. The dielectric materials modify the resonance frequency shifting by interfering with the sensor's electric field distribution. The effective inductance and capacitance values of the circuit are augmented by the material under test. Table 2 shows the comparative outcomes for simulated and measured findings.

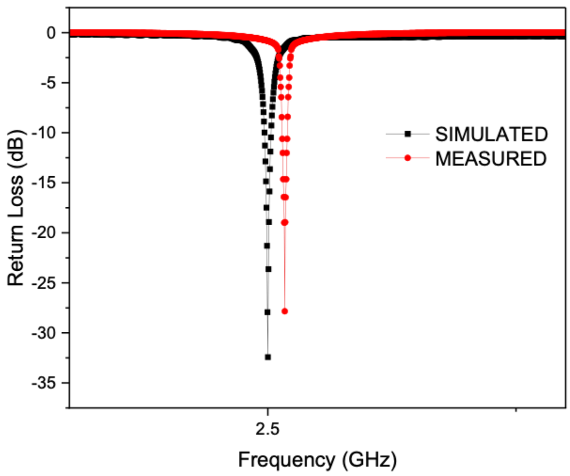

Figure 7. Simulation vs measured without MUT at 2.5 GHz

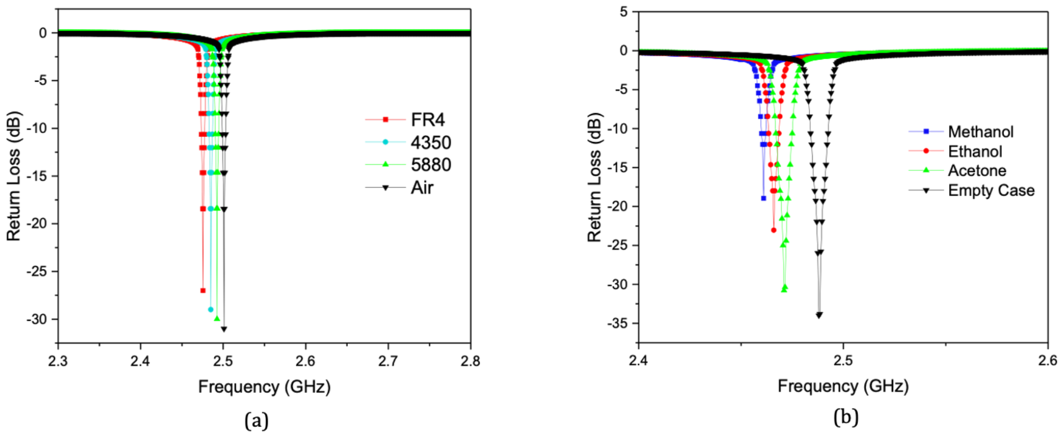

Figure 8. Simulation results with MUT (a) SUT (b) LUT

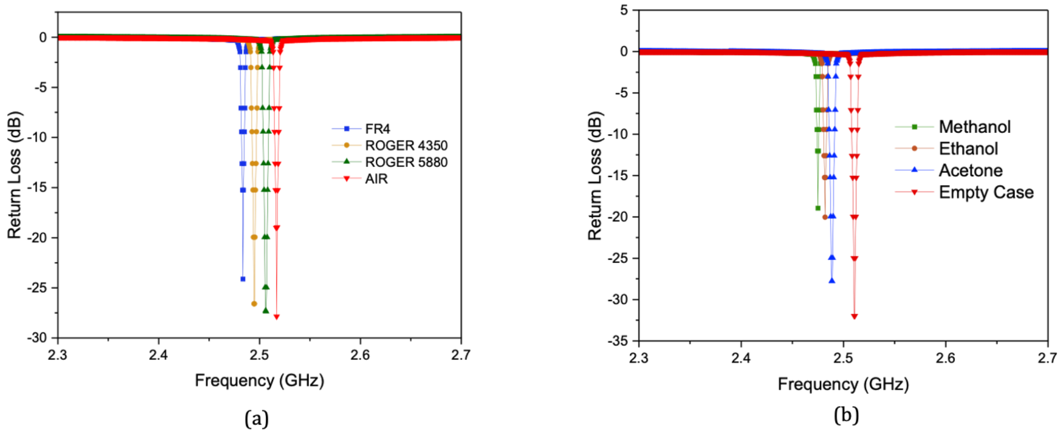

Figure 9. Measured results with MUT (a) SUT (b) LUT

Table 2. The comparison of datasets for simulation and measured results of SSRR for solid and liquid materials

MUT		**Ref. (ε')**	**f (GHz)**		**Δf (GHz)**		**S_{11} (dB)**		**Q-factor**	
Solid	Air	1	2.501	2.517	-	-	-32.420	-27.485	350	430
	Roger 5880	2.2	2.493	2.507	0.008	0.010	-31.386	-27.364	289	410
	Roger 4350	3.48	2.485	2.495	0.016	0.022	-29.975	-26.589	276	370
	FR4	4.4	2.476	2.483	0.025	0.034	-27.955	-24.115	209	250
Liquid	Without case	-	2.5	2.517	-	-	-32.420	-22.485	350	430

MUT		Ref. (ε')	f (GHz)		Δf (GHz)		S_{11} (dB)		Q-factor	
	Empty case(Air)	1	2.488	2.511	0.012	0.006	-33.979	-31.979	225	325
	Acetone	20.7	2.471	2.489	0.029	0.028	-30.785	-29.785	195	307
	Ethanol	24.5	2.466	2.482	0.034	0.035	-23.042	-20.042	152	215
	Methanol	32.7	2.461	2.475	0.039	0.042	-18.943	-18.943	138	160

5.2 Analysis of Dielectric Constant and Tangent Loss Analysis

A frequency shift is generated by an interaction between the MUT's permittivity and maximal intensity of electric fields. The experimental permittivity value for the MUT was determined using the polynomial fitting method. The percentage error trend line was used to assess the disparity between both the measurement and reference permittivity. The frequency-dependent loss tangent produces a loss that is proportional to frequency. Tangent loss values that are lower than average have a greater impact on peak amplitude. The S_{11} parameter therefore decreases when the tangent loss value is the lowest. As a result of incorrectly coupled port couplings and fabrication process losses, radiation loss that may occur in both the input and output port networks lowers the Q-factor of insertion loss. Table 3 compares the values of permittivity and loss tangent for reference and measurement to give an overview of the findings. Table 4 compares the improvement in this sensor performance with the existing literature.

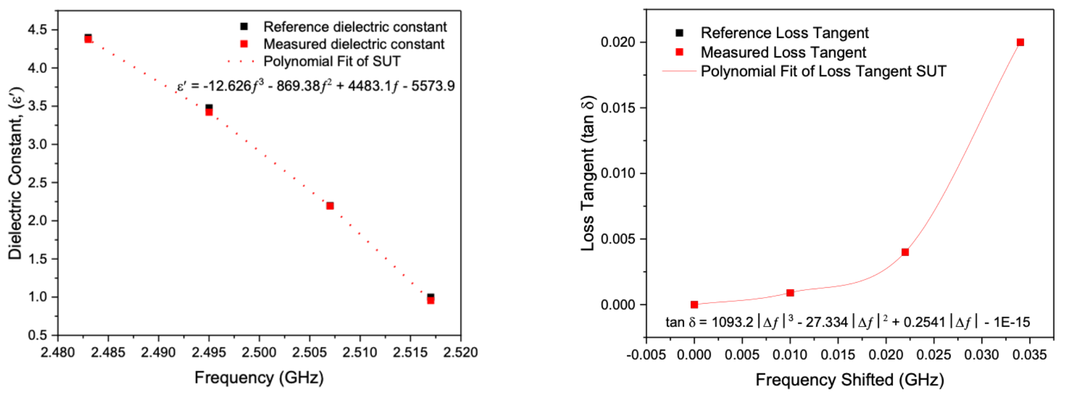

(a) (b)

Figure 10. (a) Dielectric constant of SUT (b) Loss tangent of SUT

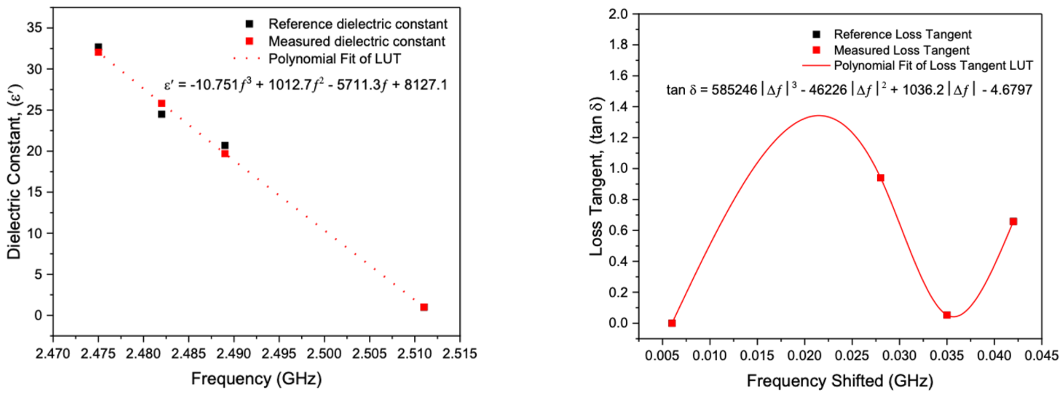

(a) (b)

Figure 11. (a) Dielectric constant of LUT (b) Loss tangent of LUT

Table 3. The comparison of complex permittivity and loss tangent of SSRR for solid and liquid materials

Types of Materials	Mut	Ref. value			SSRR					
		ε'	ε''	$\tan\delta$	ε'	ε''	$\tan\delta$	error%		
								ε'	ε''	$\tan\delta$
Solid	Air	1	0	0	0.9559	0	0	4.41	0	0
	Roger 5880	2.2	0.00198	0.0009	2.1927	0.0019741	0.00090034	0.33	0.29	0.04
	Roger 4350	3.48	0.01392	0.004	3.4223	0.0137	0.00400057	1.65	1.58	0.01
	FR4	4.4	0.0088	0.002	4.3743	0.008752	0.00200087	0.58	0.54	0.04
Liquid	Air	1	0	0	1.0101	0.000023	0.0002228	1.01	0	0
	Acetone	20.7	1.1178	0.054	19.6966	1.04139	0.052872	4.84	6.83	2.08
	Ethanol	24.5	23.0545	0.941	25.8315	24.2825	0.940036	5.43	5.32	0.10
	Methanol	32.7	21.5493	0.0659	32.0578	21.0857	0.657741	1.96	2.15	0.19

Table 4. Comparison with previous sensor

Author	Sensing Element	Material Under Test (MUT)	Frequency (GHz)	S_{11}/ S_{21} (dB)	Q-factor	%Accuracy
(Asad *et al.*, 2017)	Slotted Ring Resonator (SRR)	Biological	9	-6.2	118	70
(Ismail *et al.*, 2018)	Rectangular Microwave Resonator Sensor	Solid	4	-6.357	174	92
(Zahertar, Dodd and Torun, 2019)	Rectangular Split Ring Resonator	Liquid	2.07	-35	207	80
(Ivanov *et al.*, 2019)	Planar sensor based on two coupled rings	Oil	4-6	-6	232	87
(Oliveira *et al.*, 2020)	Complementary Split Ring Resonator (CSRR)	Soil	3.1	-22.8	225	89.95
(Al-behadili, Petrescu and Mocanu, 2020)	Complementary Split Ring Resonator	Solid	1.73-3.4	-24	295	86.9
(Ma *et al.*, 2021)	Split Ring Resonator (SRR)	Liquid	4.85-5.15	-16	52.75	50
(Amiruddin, Abdullah and Mohd, 2021)	Split Ring Resonator	Solid	2-6	-24	215	88
(Zapata-Londoño *et al.*, 2021)	Differential microwave sensor based on microstrip line loaded SRR	Differential material	3	-16	70.15	60

Author	Sensing Element	Material Under Test (MUT)	Frequency (GHz)	S_{11}/ S_{21} (dB)	Q-factor	%Accuracy
(Shahzad *et al.*, 2022)	Double Slit Complementary Square Ring Resonator (DS-CSRR)	Coal powder	2-6.5	-40.5	220	83.5
(Jang and Yang, 2022)	Double Split Ring Resonator	Solid and Liquid	2.45	-25	255	89
(Islam *et al.*, 2022)	Novel Metamaterial Triple Circle Split Ring Resonator (SRR)	Liquid	8-12	-8	135	68.5
This Work	Square Split Ring Resonator Sensor	Solid and Liquid	2.5GHz in the range 1-4 GHz	-27.85	430	98.59

6. CONCLUSION

This research led to the development of an SSRR sensor that demonstrated potential for characterising several samples of both solid and liquid materials through a single port network. Thus, the high-sensitivity and accurate sensor operates at 2.5GHz. This sensor works well and has a high Q-factor of 430. A mathematical model was created to ascertain the MUT's dielectric loss and the dielectric characteristics. The dielectric characteristics of the material were determined through polynomial curve fitting. Both the measurement error for permittivity and the loss tangent error are within 2%. This sensor can be used in industrial and commercial applications to verify the quality and safety of foods and pharmaceuticals because its accuracy rate is greater than 98.59%. Because this sensor only needs a tiny amount of sample to be analysed, it has the advantage of being more dependable. Each piece of data has been noted along with its dielectric properties, Q-factor, return loss, and resonant frequency.

Acknowledgments

The author would like to thank the Centre for Research and Innovation Management (CRIM) UTeM, Universiti Teknikal Malaysia Melaka (UTeM), and the Malaysian Ministry of Higher Education (MOHE) for financing this work under RACER/2019/FKEKK-CETRI/F00406.

REFERENCES

[1] Al-Behadili, A.A. et al. , **Modified split ring resonators sensor for accurate complex permittivity measurements of solid dielectrics**, Sensors (Switzerland), 2020 20(23), pp. 1–18. doi:10.3390/s20236855.

[2] Al-behadili, A.A., Petrescu, T. and Mocanu, I.A. , **Complimentary split ring resonator sensor with high sensitivity based on material characterization**', Telkomnika (Telecommunication Computing Electronics and Control), 2020 18(1), pp. 272–281. doi:10.12928/TELKOMNIKA.v18i1.13255.

[3] Alahnomi, R.A. et al. , **Enhanced symmetrical split ring resonator for metallic surface crack detection**', Telkomnika (Telecommunication Computing Electronics and Control), 2019, 17(4), pp. 2107–2115. doi:10.12928/TELKOMNIKA.v17i4.12939.

[4] Narayanan PM, **Microstrip transmission line method for broadband permittivity measurement of dielectric substrates**, *IEEE Trans. Microw. Theory Tech*, 2014;62:2784–90.

[5] Alhegazi, A. et al. , **Analysis and investigation of a novel microwave sensor with high Q-factor for liquid characterization**', Telkomnika (Telecommunication Computing Electronics and Control), 2019, 17(2), pp. 1065–1070. doi:10.12928/TELKOMNIKA.V17I2.11901.

[6] Amiruddin, A.A.M., Abdullah, N. and Mohd, E. , **Development of split ring resonator for pineapple moisture content detection**', Bulletin of Electrical Engineering and Informatics, 2021, 10(5), pp. 2636–2642. doi:10.11591/eei.v10i5.2828.

[7] Mohd Bahar AA, Zakaria Z, Md. Arshad MK, Isa AAM, Dasril Y, Alahnomi RA, **Real Time Microwave Biochemical Sensor Based on Circular SIW Approach for Aqueous Dielectric Detection. Sci. Rep**, [Internet] 2019;9:1–12, Available from: http://dx.doi.org/10.1038/s41598-019-41702-3.

[8] Islam, R. et al. , **Metamaterial sensor based on rectangular enclosed adjacent triple circle split ring resonator with good quality factor for microwave sensing application**', Scientific Reports, 2022, pp. 1–18. doi:10.1038/s41598-022-10729-4.

[9] Ivanov, A. et al. , **Design and characterization of a microwave planar sensor for dielectric assessment of vegetable oils**', Electronics (Switzerland), 2019, 8(9), pp. 1–9. doi:10.3390/electronics8091030.

[10] Ismail, M.K. et al. , **Microwave planar sensor for determination of the permittivity of dielectric material**', Bulletin of Electrical Engineering and Informatics, 2018, 7(4), pp. 640–649. doi:10.11591/eei.v7i4.1355.

[11] Jang, S.-Y. and Yang, J.-R. , **Double Split-Ring Resonator for Dielectric Constant Measurement of Solids and Liquids**', Journal of Electromagnetic Engineering and Science, 2022, 22(2).

doi:10.26866/jees.2022.2.r.68.

[12] Lee, G.H. et al. , **Generalized Design Technique of Ultra-Wideband Transitions for Quasi-TEM Planar Transmission Lines Based on Analytical Models**', IEEE Access, 2021, 9, pp. 52619–52633. doi:10.1109/ACCESS.2021.3069870.

[13] Iqbal A, Smida A, Saraereh OA, Alsafasfeh QH, Mallat NK, Lee BM, **Cylindrical dielectric resonator antenna-based sensors for liquid chemical detection**, *Sensors (Switzerland)*, 2019;19:2–10.

[14] Yeo J, Lee JI, **Slot-loaded microstrip patch sensor antenna for high-sensitivity permittivity characterization**, *Electron*, 2019;8.

[15] Ma, J. et al. , **Complex permittivity characterization of liquid samples based on a split ring resonator (SRR)**', Sensors, 2021, 21(10). doi:10.3390/s21103385.

[16] Mahashabde, S. et al. , **Fast Tunable High- Q -Factor Superconducting Microwave Resonators**', Physical Review Applied, 2020, 10(1), p. 1. doi:10.1103/PhysRevApplied.14.044040.

[17] Muñoz-Enano, J. et al. , **Planar microwave resonant sensors: A review and recent developments**', Applied Sciences (Switzerland), 2020, 10(7). doi:10.3390/app10072615.

[18] Oliveira, J.G.D. et al. , **CSRR-based microwave sensor for dielectric materials characterization applied to soil water content determination**', Sensors (Switzerland), 2020, 20(1). doi:10.3390/s20010255.

[19] Rahman, N.A. et al. , **Dual band planar microwave sensor for dielectric characterization using solid and liquid sample**', Journal of Telecommunication, Electronic and Computer Engineering, 2018, 10(2–8), pp. 27–32.

[20] Raveendran, A. et al. , **Complex Permittivity Extraction of Planar Dielectrics Using a Noninvasive Microwave Transmission Line Resonant Technique**', 2021, 70.

[21] Reyes-Vera, E. et al. , **A submersible printed sensor based on a monopole-coupled split ring resonator for permittivity characterization**', Sensors (Switzerland), 2019, 19(8). doi:10.3390/s19081936.

[22] Shahzad, W. et al. , **A Low-Cost Metamaterial Sensor Based on DS-CSRR for Material Characterization Applications**', Sensors, 2022, 22(5), pp. 1–11. doi:10.3390/s22052000.

[23] Sobkiewicz, P., Bieńkowski, P. and Błażejewski, W. , **Microwave non-destructive testing for delamination detection in layered composite pipelines**', Sensors, 21(12), 2021. doi:10.3390/s21124168.

[24] Su, L. et al. , **Analytical method to estimate the complex permittivity of oil samples**', Sensors (Switzerland), 2018, 18(4), pp. 1–12. doi:10.3390/s18040984.

[25] Pozar D, **Microwave Engineering Fourth Edition. John Wiley & Sons Ltd**, 2005.

[26] Wang, C. et al. , **A Sensor for Characterisation of Liquid Materials with High Permittivity and High Dielectric Loss**', Sensors, 2022, 22(5), pp. 1–14. doi:10.3390/s22051764.
[27] Xu, K. et al. , **Novel Microwave Sensors Based on Split Ring Resonators for Measuring Permittivity**', IEEE Access, 2018, 6(c), pp. 26111–26120. doi:10.1109/ACCESS.2018.2834726.
[28] Zahertar, S., Dodd, L.E. and Torun, H. , **Embroidered Rectangular Split-Ring Resonators for Material Characterisation**', FLEPS 2019 - IEEE International Conference on Flexible and Printable Sensors and Systems, Proceedings, 2019, 2, pp. 2–4. doi:10.1109/FLEPS.2019.8792233.
[29] Zapata-Londoño, J. et al. , **Differential microwave sensor based on microstrip lines loaded with a split-ring resonator for dielectric characterization of materials**', Journal of Physics: Conference Series, 2118(1), 2021. doi:10.1088/1742-6596/2118/1/012004.